# Spatial instabilities in a cloud of cold atoms

Rudy Romain,[*] Antoine Jallageas,[†] Philippe Verkerk, and Daniel Hennequin[‡]
*Université Lille, CNRS, UMR 8523–PhLAM–Physique des Lasers Atomes et Molécules, 59000 Lille, France*
(Received 26 February 2016; published 11 November 2016)

Cold atomic clouds have been shown to have some similarities with plasmas. Previous studies showed that such clouds exhibit instabilities induced by long-range interactions. However, they did not describe the spatial properties of the dynamics. In this paper, we study experimentally the spatial nature of stochastic instabilities, and we find out that the dynamics is localized. Data are analyzed both in the spectral domain and in the spatial domain (principal component analysis). Both methods fail to describe the dynamics in terms of eigenmodes, showing that space and time are not separable.

DOI: 10.1103/PhysRevE.94.052212

During the past few decades, cold atoms have proven to be more than an extraordinary tool for studying the physics of dilute matter. Many spectacular results concern the field of condensed matter, such as, e.g., the direct observation of Anderson localization [1], or that of the BEC-BCS crossover [2]. However, in the field of dilute matter, important questions remain unresolved. In particular, magneto-optical traps (MOTs) exhibit instabilities, observed for several decades, usually seen as a source of nonrepeatability for further use of cold atomic samples. These instabilities have been studied for 15 years on their own, but the detailed mechanisms responsible for their appearance have not been clearly identified yet [3–11]. In that context, cold atoms are often compared to plasmas, and they are even thought to be a good model system for plasmas, in particular because experiments are considered to be relatively simple and well-controlled [7].

Indeed, although cold atoms in a MOT are neutral, it has been demonstrated that a Coulombian-like repulsive force appears in the multiple scattering regime. In an optically thick cloud, a photon can undergo several scattering events before escaping the cloud. A single emission and absorption event induces the same momentum kick for the two atoms, but in the opposite direction, resulting in an exclusively repulsive interaction. This process creates a Coulombian-like force as the flux of photons varies like the inverse of the squared distance from the emitter [12]. This long-range interaction plays a crucial role in the behavior of a cold atom cloud, as it also prevents high atomic densities and thus any other type of atomic interactions. Because of these long-range interactions, fluid-dynamical models used to describe cold atoms physics have been adapted from plasma physics [8,10,11]. On the other hand, it has been demonstrated that the dynamics of cold atoms in a MOT can be described through the Vlasov-Fokker-Planck equation [9], such as, e.g., the plasma dynamics in the inertial confinement fusion [13], the stellar dynamics [14], or the electron dynamics in storage rings [15].

Most of these systems are known to exhibit instabilities under appropriate parameter sets. Numerous types of instabilities have been observed, with very different properties and signatures [13–17]. Although plasmas are governed by long-range interactions, instabilities appear not only at large spatial scales but also at smaller scales. Some examples of local instabilities are the microbunching instability in the storage rings [15], drift wave microinstabilities in plasmas confined by a magnetic field [16], or microinstabilities of the solar corona [17].

Mainly two types of instabilities have been reported through cold atoms experiments. Self-sustained instabilities are periodic oscillations [4,7], while stochastic instabilities exhibit random characteristics [3]. In all cases, the experimental characterization was done through the temporal evolution of global variables, such as the fluorescence of the cloud or the location of its center of mass. The spatial properties of the instabilities, in particular their location in the cloud, are not known. However, most simplified models allowing these instabilities to be reproduced have considered them to be global [5,6]. On the other hand, taking formally into account the different processes involved in the MOTs leads to the Vlasov-Fokker-Planck equation, implicitly predicting local instabilities [9]. Models derived from plasmas also predict local phenomena, such as photon bubbles [10], but none of them has been observed yet. Thus gaining knowledge on the spatiotemporal characteristics of the cloud dynamics appears to be crucial to know which methods and approximations can be used to solve the full set of equations describing the MOT. It could also help to clarify the similarities between cold atom instabilities, hydrodynamics turbulence, and plasma instabilities.

We report in this paper the experimental observation of local instabilities through a detection setup that allowed us to record the spatiotemporal evolution of the atoms in the MOT. We focus here on the previously observed stochastic instabilities [3,5], and we show that these instabilities are localized in a limited area of the cloud. The analysis of the dynamics by two different methods does not give results consistent with the hypothesis of global temporal or spatial motion. The paper is organized as follows: after a brief description of the experimental setup, we analyze the dynamics of the MOT through global tools, as used in the literature,

[*]Present address: Department of Physical Sciences, The Open University, Walton Hall, MK7 6AA Milton Keynes, United Kingdom.
[†]Present address: Laboratoire Temps–Fréquence, Institut de Physique, Université de Neuchâtel, Avenue de Bellevaux 51, 2000 Neuchâtel, Switzerland.
[‡]Author to whom all correspondence should be addressed: daniel.hennequin@univ-lille1.fr; Permanent address: Laboratoire PhLAM Bâtiment P5–Université Lille, 59655 Villeneuve d'Ascq Cedex, France.

 

in order to clearly establish the type of instabilities we are studying. Then we analyze the dynamics through two methods: local temporal analysis gives information on the motion eigenfrequencies, while principal component analysis (PCA) allows us to identify spatial eigenmodes.

Our experimental setup is described in detail in [3–6]. We use a standard Cs MOT with three retroreflected beams. However, special care is taken with regard to the stability of parameters that could introduce artefacts in the dynamics. For example, we use a single-mode optical fiber to clean the transverse profile of laser beams. We also modulate the relative phases of all the beams to avoid possible interference patterns. The modulation frequency ($>1$ kHz) is chosen larger than the collective atomic response frequencies so that the intensity is averaged [18]. These two features prevent any local variation of the laser intensity. The MOT produces a cloud of cold atoms with a typical diameter of 4 mm and a typical density of $10^9$ atoms/cm$^3$. These values are characteristic of the multiple scattering regime in which the collective effects play a key role in the behavior of the cloud [19]. To obtain the desired dynamical regime, we adjust two control parameters: (i) the intensity $I$ of a single incoming beam, expressed in units of the saturation intensity $I_{\rm sat} = 1.1\,{\rm mW\,cm^{-2}}$ ($D_2$ line of $^{133}$Cs), and (ii) the detuning $\Delta$ between the laser frequency and the atomic transition, expressed in units of the natural linewidth $\Gamma = 2\pi \times 5.22\,{\rm MHz}$. In the following, all the illustrations and examples correspond to $I = 11 I_{\rm sat}$ and $\Delta = -1.8\Gamma$. They are typical of the dynamics observed for $10 I_{\rm sat} \leqslant I \leqslant 15 I_{\rm sat}$ and $-1.9\Gamma \leqslant \Delta \leqslant -1.6\Gamma$ [5,6].

The spatiotemporal dynamics of the atoms is analyzed by recording the local temporal evolution of the fluorescence at any point of the cold atom cloud. Let us remember that the number of atoms is proportional to the fluorescence for a given set of MOT parameters. As during an acquisition the MOT parameters are kept constant, we thus record the spatiotemporal evolution of the atomic density in the cloud.

It has been shown that instabilities exhibit frequencies ranging from 1 to 100 Hz [3–6]. Thus to record the dynamics, a standard video camera at 30 frames per second is not adapted. We use a fast video camera (Phantom v7.3 camera from Vision Research) that can record up to 10 000 frames/s. A set of lenses is used to cover an optical field of $15 \times 10$ mm and a depth of field of 2.5 mm, well fitting the cloud size. An important point is to determine if the light recorded by such a camera comes only from the surface of the cloud, or from any point inside the cloud. Instabilities arise when the atomic density is high enough, i.e., when the collective nonlinear processes inside the cloud cannot be neglected [3–6]. However, even for such relatively dense clouds, the number of scattering events for most photons escaping the cloud is one or two [18]. That means that the camera captures photons coming from any point inside the cloud, but with a different weight depending on the location. This last point has to be kept in mind, although it has marginal consequences on the interpretation of the pictures. Indeed, the main difficulty is that we record a two-dimensional (2D) projection of the cloud, while the dynamics occurs in three dimensions. This makes the interpretation of the records harder.

The location of the camera is dictated by the preferential direction of the dynamics. Let us call $Ox$, $Oy$, and $Oz$ the three perpendicular axes corresponding to the three incident beams of the trap, $Oz$ being also the axis of the coils. Thanks to the choice of a retroreflecting beam configuration, and because of the shadow effect [3–6], the amplitude of the dynamics is enhanced in a direction along the line $x = y = 2z$. Looking at the dynamics along this direction would lead to artifacts masking some parts of the dynamics. The camera axis, also imposed by the available space on the setup, is chosen close to the $(x = y, z = 0)$ direction. In that way, the preferential direction of the dynamics projects with an angle of 20° on the picture plane, leading to a satisfactory resolution of the observations.

To make the link between the present work and the previous reported observations, we also use a 4-quadrant photodiode (4QP) to monitor the total cloud fluorescence and the position of the cloud center of mass, as, e.g., in [4]. The signals from the 4QP and the pictures from the video camera are recorded synchronously.

As pointed out above, we focus here on the regime of stochastic instabilities. This regime has been studied in detail in several papers, both experimentally and theoretically [3,5]. Experimental data consisted of time sequences of the total number $N$ of atoms in the cloud and of the location $r$ of its center of mass. Note that the spatial distribution of the atoms in the cloud was not accessible. The dynamics has been shown to consist essentially of erratic fluctuations of $N$ and $r$. It was demonstrated that these fluctuations were not deterministic chaos. However, this noisy dynamics is cut off with bursts of periodic oscillations at a frequency that does not appear outside the bursts. This behavior resembles fluid intermittency, but this hypothesis does not stand up to examination. Indeed, the amplitude of the oscillations depends on the MOT parameters: in particular, it exhibits a maximum as a function of $\Delta$. This system has been modeled with rate equations of $N$ and $r$, which allow the main characteristics of the observations to be reproduced. The whole dynamics has been shown to be induced by a stochastic resonance, which fixes in particular the parameters where the instabilities are stronger.

In the present work, the unstable regime shows the same characteristics as in [3]. In particular, for the parameters given above, instabilities are maximal for $\Delta = -1.8\Gamma$; the dynamics (the number of atoms and the center of mass) is a succession of regular bursts and noisy intervals (Fig. 1); in the bursts, a frequency $\omega_1 \simeq 2\pi \times 21\,{\rm Hz}$ dominates the dynamics. To be more exhaustive than the previous studies, we also study the characteristics of the secondary frequency components. In the burst regime, the second component $\omega_2 \simeq 2\pi \times 72\,{\rm Hz}$ is two orders of magnitude smaller than $\omega_1$. The components $2\omega_1$ and $\omega_2 - \omega_1$ are also present, with amplitudes similar to that of $\omega_2$. In the noisy intervals, $\omega_2$ is present, with the same amplitude as in the bursts. $\omega_1$ is also present, but with an amplitude smaller than $\omega_2$. In summary, $\omega_1$ appears mainly inside the bursts, while $\omega_2$ is always present. The values of $\omega_1$,$\omega_2$ and their harmonics are in agreement with those observed in previous studies, and they are also close to the plasmalike frequency introduced in [7]. Moreover, these values appear as a robust characteristic of the instabilities. On the whole interval of the MOT parameters—detuning and laser intensity—where the instabilities appear, they can be considered to be constant as

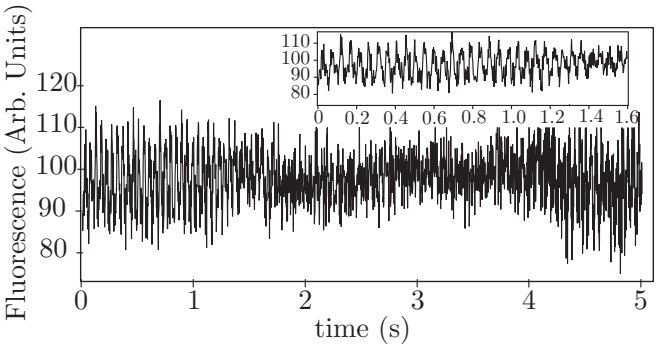


FIG. 1. Dynamics of the total number of atoms $N$, recorded through the total fluorescence collected by the 4QP, for $\Delta = -1.8\Gamma$ and $I \simeq 13 I_{\text{sat}}$. This example shows a sequence starting with a periodic burst followed by erratic fluctuations. The inset is a zoom of the periodic burst.

they vary less than 4% while the amplitude of the dynamics varies by several orders of magnitude.

For this study, our aim is to characterize the nature—space-dependent or not—of the dynamics. Thus we do not need to record long time series with a good time resolution, as would be necessary for, e.g., making a topological analysis of the dynamics attractors. We only need to follow the usual rules of frequency analysis, i.e., to record at least two points per period. The following results correspond to 512 × 512 pixel pictures recorded with a rate of 400 frames/s. The length of the analyzed sequences is 625 ms, i.e., 250 frames, corresponding to the typical length of the bursts.

To determine the spatial dependence of the dynamics, a straightforward approach consists in applying the frequency analysis used previously to each point of the cloud. Figure 2 shows a typical result for the dynamics inside a burst. In Figs. 2(a) and 2(b), the cloud of cold atoms is shown through a contour plot of its averaged fluorescence. In Fig. 2(a), we represent in gray levels the amplitude of the $\omega_1$ component in each point of the cloud, obtained by fast Fourier transform (FFT) of each pixel of the picture sequence. It appears certain that the dynamics depends on the space. Instabilities appear in two small areas of the cloud, covering about 10 % of the whole cloud. The two areas have very different shapes and sizes, and we see two local maxima in one of the areas. Figure 2(c) shows that the two areas pulse with opposite phases. It is difficult to deduce from such 2D observations the exact 3D dynamics, but it is clear that the instabilities consist of a local pulsation or rotation, while the rest of the cloud is stable.

The above example is typical of what we observed in all the recorded sequences. The instabilities are always localized in a limited area of the cloud, covering typically 10% of the whole cloud. Nevertheless, some differences appear from one sequence to another. The most noticeable changes in time are the location of the local maxima and their number as well as their shape, which appear to be nontrivial.

We performed the same analysis for the $\omega_2$ component, and we found the same type of results as for the $\omega_1$ component: the instabilities are localized in a relatively small area, and they correspond to a motion of pulsation or rotation of a part of the cloud. As discussed above, inside the bursts, the $\omega_2$ component is small as compared to the $\omega_1$ component, making the data analysis less reliable. However, it appears clear that in this case, the characteristics of the $\omega_2$ component follow those of the $\omega_1$ component, delimiting the same unstable area with the same type of motion. Figures 2(b) and 2(d) show, respectively, the amplitude and the phase of the $\omega_2$ component for the same burst as in Figs. 2(a) and 2(c): the spatial distributions of the instabilities are the same for the two components. The similarity of the phase distributions is less convincing, due to the weakness of the component, but in spite of that, a phase opposition appears between the two areas. To generalize this observation, we computed the spatial overlap between the two components for all the recorded sequences, and we found that they have in most cases a similar spatial distribution.

Outside the bursts, the $\omega_2$ component is still present and has the same characteristics. But as its spatial distribution cannot be compared to that of $\omega_1$, and because of the poor signal-to-noise ratio of this regime, the results are less relevant than in the regime inside the bursts.

Thus the dynamics appears to be a small (in space) and weak (in amplitude) periodic motion of a small part of the cloud at the $\omega_2$ frequency, cut off by bursts where the amplitude of the motion increases temporarily, while its main frequency shifts to $\omega_1$. However, this description is not completely satisfactory. Indeed, it gives information about the temporal components of the dynamics, but it does not give any information about the spatial components. In particular, it seems to associate one spatial component with two different frequencies, while in spatiotemporal systems where the temporal dynamics and the space distribution can be separated, such as, e.g., in multimode lasers [20], a spatial eigenmode is associated with only one eigenfrequency. In the following, we adopt another approach.

PCA has the advantage of providing a description of the dynamics of the system without requiring any preliminary hypothesis. The dynamics is described in terms of a superposition of spatial modes, giving complementary information with respect to the Fourier analysis. The analysis is performed using the method described in [21].

The result of the PCA is a set of spatial modes forming a basis whose size is equal to the number of pictures of the sequence (250 in our case). If these modes are sorted according to their weight, i.e., their contribution to the total statistical deviation around the averaged atomic distribution, the method leads to the determination of the number of modes useful to describe the dynamics. In our case, we find that in the sequences considered here, the main mode contains between 50% and 80% of the statistical fluctuations, and the second mode between 5% and 25%. Thus the dynamics appears to be dominated by one single mode, although the weight of the second mode is not negligible. Depending on the desired accuracy, the third mode, with a weight of 10% ± 5%, could be taken into account. In the following, we consider only the first two modes.

Figure 3 shows the first two modes obtained by the PCA of the sequence of Fig. 2. Note the similarity of the main mode with the $\omega_1$ spatial distribution [Fig. 2(a)]. However, this result is not general. On the contrary, we observe a major difference between the modes given by the PCA and those resulting from the Fourier analysis. While in the latter a wide variety of shapes are obtained, the results are more homogeneous in

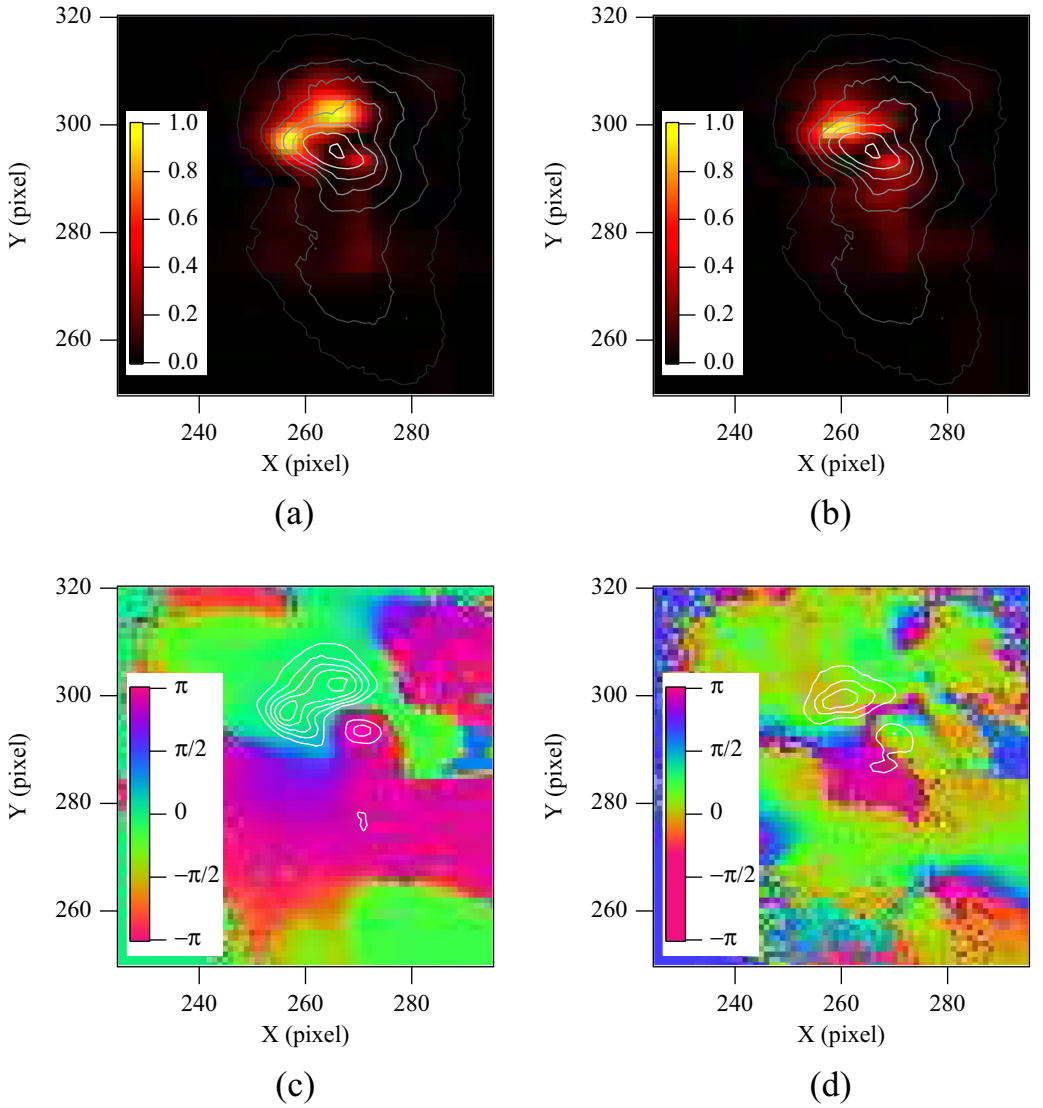


FIG. 2. Spatial distribution of instabilities for one sequence: (a) and (b) show the local amplitude of the two main components: $\omega_1$ and $\omega_2$. The normalized magnitude squared of the spectral component is represented in gray level. The contour plot shows the averaged fluorescence during the sequence. The contour interval is equal to 12.5% of the maximum (the point corresponding to the 100% contour line is not shown). Parts (c) and (d) represent the corresponding phase distributions. Grayscale represents the relative phase of the local oscillation between $\pm\pi$. The contour plot identifies the unstable areas.

the former. In fact, one set of modes dominates the whole dynamics. This basis—let us call it the main basis—is not the only one found by the PCA, but it is the most frequent in the set of recorded sequences. This regime is randomly interrupted by short intervals where the dynamics is described by another basis before it returns to the main basis. These alternative bases differ from one sequence to another, and we did not find any common properties. For example, in a few cases the modes of the main basis appear, but in a different order: the first mode of the main basis becomes the second mode of the basis.

A surprising result is that the regimes found with the PCA do not correspond to those given by the Fourier analysis. In particular, the sequences described by the main basis do not follow the succession of bursts and noisy intervals. As a consequence, the frequencies associated with the main basis may change from one sequence to another. Moreover, the time evolution of a given spatial mode may exhibit different frequencies in different sequences. Figure 4 shows the time evolution and the FFT of two modes dominating the dynamics in two consecutive sequences. Although the two modes are similar, they are associated with two very different time evolutions: for the first one, both frequencies $\omega_1$ and $\omega_2$ drive the dynamics, while the second one corresponds to a burst where $\omega_1$ dominates the dynamics.

In summary, the PCA leads to a description of the dynamics in terms of spatial modes. The results show that such a description is as relevant as the description in terms of frequency components. Two regimes are found: the first one corresponds to a well-identified spatial mode basis, referred to as the main basis, and the second one is described by different bases. From this point of view, the description obtained by the PCA is similar to that of the Fourier analysis. But surprisingly,

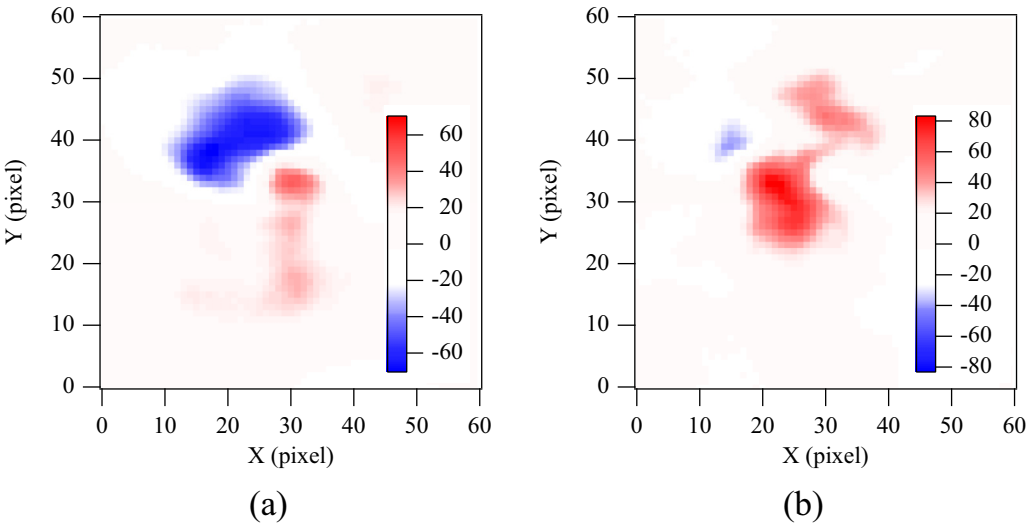


FIG. 3. Two first spatial modes given by the PCA [(a) and (b), respectively] for the same sequence as in Fig. 2. In both cases, the spatial distribution is represented in absolute value in gray level, and the upper and lower areas have to be understood, respectively, as an excess (in blue) and a depletion of atoms (in red). This information is similar to that given by the phase of the Fourier analysis.

the two regimes of the PCA do not correspond in time sequences to the two regimes of the Fourier analysis.

The two approaches—temporal and spatial—give complementary information on the dynamics: the dynamics of the cloud of cold atoms in a MOT is a genuine spatiotemporal system, where the spatial and temporal behaviors cannot be separated. This result implies that an exclusively temporal description as in [3–7] must be abandoned. However, we must not forget that the temporal model in [5] was able to reproduce qualitatively the observed dynamics. A naive interpretation

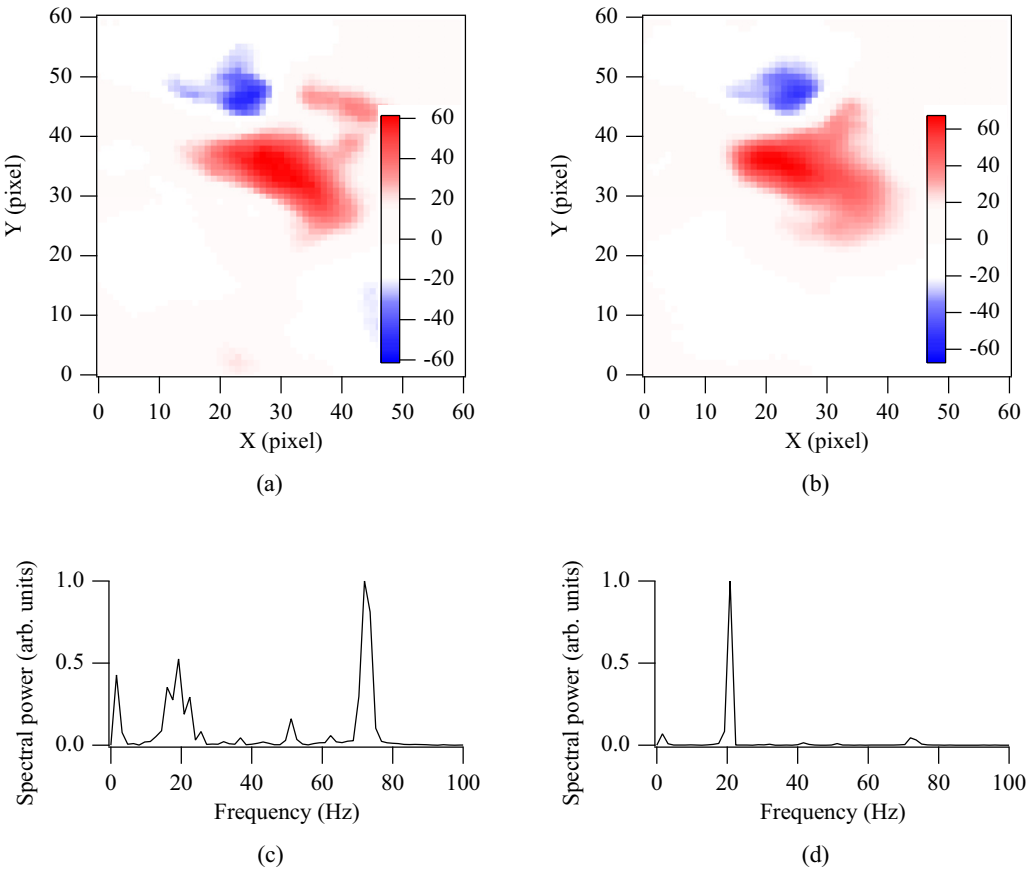


FIG. 4. From top to bottom: first modes calculated by the PCA for two consecutive sequences and the FFT of the time evolution of these modes.

could be that only a spatial subset of the atoms undergoes temporal instabilities as described in [5], while the rest of the cloud is stationary. In addition to the above arguments, at least two points show that this interpretation is not correct: the spatial distribution of the unstable area is not always the same for a given set of parameters, and most importantly, the PCA shows that at least two spatial modes are required to describe the dynamics. Thus the dynamics studied here has all the characteristics of spatial stochastic resonance [22].

As discussed in the introduction, several models have been proposed to describe the MOT dynamics. Until now, none of these models has been able to show stochastic resonance, but their numerical solutions have been explored very incompletely. However, one of the generic systems modeling stochastic resonance is governed by the Fokker-Planck equation [22]. Therefore, the model developed in [9], which leads to the Vlasov-Fokker-Planck equation, is likely to generate such a mechanism. Moreover, in this model built formally from the different processes involved in the MOTs, the collective effects appear through spatial derivatives, and thus they could produce local dynamics. Thus, although numerical solutions for this model are not yet available, it is a good candidate to describe the dynamics discussed here.

We report in the present paper experimental results on the dynamics of an unstable cloud of cold atoms in a regime of stochastic instabilities. Previous studies focused on the temporal behavior of the instabilities. Here we study both the spatial and temporal properties of the dynamics. Although the atomic motion cannot be clearly identified, as our analysis is based on a 2D projection of a 3D motion, we show that the oscillations are localized in space. We analyze the dynamics through two different methods, and both point out the key role of space in the dynamics. Moreover, the analyses in terms of frequency components and spatial modes show that the relation between the temporal regime and the spatial distribution is not straightforward, as the same spatial distribution can correspond to different temporal regimes. These results invalidate the description in terms of purely temporal models, as in [3–7], and they require the use of fully spatiotemporal models, such as the Vlasov-Fokker-Planck model [9] or the plasma-derived model [10]. To go further, in particular to know what the similarities are between cold atoms and plasma dynamics, a deep physical interpretation of the observed behavior is required. Therefore, the next step is to run numerical simulations to obtain quantitative agreement between models and experimental observations, particularly in the dynamical regimes.

*Note added*. Recently, an experimental observation related to our results was reported [23].

The authors would like to thank R. Dubessy for helpful discussions about the PCA. This work was supported by the Labex CEMPI (Grant No. ANR-11-LABX-0007-01) and "Fonds Européen de Développement Economique Régional."

[1] F. Jendrzejewski, A. Bernard, K. Müller, P. Cheinet, V. Josse, M. Piraud, L. Pezzé, L. Sanchez-Palencia, A. Aspect, and P. Bouyer, Nat. Phys. **8**, 398 (2012).
[2] T. Bourdel, L. Khaykovich, J. Cubizolles, J. Zhang, F. Chevy, M. Teichmann, L. Tarruell, S. J. J. M. F. Kokkelmans, and C. Salomon, Phys. Rev. Lett. **93**, 050401 (2004).
[3] D. Wilkowski, J. Ringot, D. Hennequin, and J. C. Garreau, Phys. Rev. Lett. **85**, 1839 (2000).
[4] A. di Stefano, M. Fauquembergue, P. Verkerk, and D. Hennequin, Phys. Rev. A **67**, 033404 (2003).
[5] D. Hennequin, Eur. Phys. J. D **28**, 135 (2004).
[6] A. di Stefano, Ph. Verkerk, and D. Hennequin, Eur. Phys. J. D **30**, 243 (2004).
[7] G. Labeyrie, F. Michaud, and R. Kaiser, Phys. Rev. Lett. **96**, 023003 (2006).
[8] J. T. Mendonça, R. Kaiser, H. Terças, and J. Loureiro, Phys. Rev. A **78**, 013408 (2008).
[9] R. Romain, D. Hennequin, and P. Verkerk, Eur. Phys. J. D **61**, 171 (2011).
[10] J. T. Mendonça and R. Kaiser, Phys. Rev. Lett. **108**, 033001 (2012).
[11] J. D. Rodrigues, J. A. Rodrigues, A. V. Ferreira, and J. T. Mendonça, Opt. Quantum Electron. **48**, 169 (2016).
[12] L. Pruvost, I. Serre, H. T. Duong, and J. Jortner, Phys. Rev. A **61**, 053408 (2000).
[13] C. P. Ridgers, R. J. Kingham, and A. G. R. Thomas, Phys. Rev. Lett. **100**, 075003 (2008).
[14] P.-H. Chavanis, Phys. Rev. E **68**, 036108 (2003).
[15] E. Roussel, C. Evain, C. Szwaj, and S. Bielawski, Phys. Rev. ST Accel. Beams **17**, 010701 (2014).
[16] J. Weiland, *Stability and Transport in Magnetic Confinement Systems*, Springer Series in Atomic, Optical and Plasma Physics Vol. 71 (Springer, New York, 2012).
[17] E. Marsch, Living Rev. Solar Phys. **3**, 1 (2006).
[18] R. Romain, H. Louis, P. Verkerk, and D. Hennequin, Phys. Rev. A **89**, 053425 (2014).
[19] D. W. Sesko, T. G. Walker, and C. Wieman, J. Opt. Soc. Am. B **8**, 946 (1991).
[20] D. Hennequin, D. Dangoisse, and P. Glorieux, Opt. Commun. **79**, 200 (1990).
[21] R. Dubessy, C. De Rossi, T. Badr, L. Longchambon, and H. Perrin, New J. Phys. **16**, 122001 (2014).
[22] L. Gammaitoni, P. Hänggi, P. Jung, and F. Marchesoni, Rev. Mod. Phys. **70**, 223 (1998).
[23] J. D. Rodrigues, J. A. Rodrigues, A. V. Ferreira, H. Terças, R. Kaiser, and J. T. Mendonça, arXiv:1604.08114.